Revista Colombiana de Estadística - Applied Statistics
July 2024, volume 47, issue 2, pp. 423–451
http://doi.org/10.15446/rce.v47n2.112805

Data-Driven Modeling of Impact of Differential Efficacy of COVID-19 Vaccines in Two Socio-Economically Contrasting Cities: New York, USA and Bogotá, Colombia

Modelado basado en datos del impacto de la eficacia diferencial de las vacunas contra el COVID-19 en dos ciudades socioeconómicamente contrastantes: Nueva York, EE.UU. y Bogotá, Colombia

Erika Johanna Martínez-Salinas[1,a], Viswanathan Arunachalam[1,b], Caitlin Seibel[2,c], Yutian Huang[3,d], Jackson Reisman[4,e], Moatlhodi Kgosimore[5,f], Anuj Mubayi[6,g], Padmanabhan Seshaiyer[7,h]

[1]Department of Statistics, Faculty of Science, Universidad Nacional de Colombia, Bogotá, Colombia

[2]School of public health, University of Michigan, Michigan, United States

[3]Mathematics Department, Lafayette College, Pennsylvania, United States

[4]The College of New Jersey, New Jersey, United States

[5]Department of Biometry and Mathematics, Botswana University of Agriculture and Natural Resources, Gaborone, Botswana

[6]Center for Collaborative Studies in Mathematical Biology, Illinois State University, Illinois, United States

[7]Mathematical Sciences, George Mason University, Virginia, United States

Abstract

In an effort to curb the spread of COVID-19, various types of vaccines, including mRNA, viral vectors, and traditional ones, were globally approved and implemented. However, the distribution of vaccines in each country became a critical and determining factor in the disease's evolution. The present study aims to understand the differential impact of the different available

[a]Ph.D(c). E-mail: ejmartinezsa@unal.edu.co
[b]Ph.D. E-mail: varunachalam@unal.edu.co
[c]M.Sc student. E-mail: caitlinpseibel@gmail.com
[d]Mathematics degree. E-mail: tinahuangyt00@gmail.com
[e]Mathematics degree. E-mail: reismaj4@tcnj.edu
[f]Ph.D. E-mail: mkgosi@buan.ac.bw
[g]Ph.D. E-mail: anujmubayi@yahoo.com
[h]Ph.D. E-mail: pseshaiy@gmu.edu

vaccine types on disease burden. A proposed mathematical model considers multiple vaccines in a community to analyze the dynamics of COVID-19 transmission in two socioeconomically diverse regions. Secondary incidence data for the cities of Bogotá, Colombia, and New York, USA, from March 2020 to December 2021 were used to estimate vaccine-related parameters and actual transmission rates. The results suggest that although New York has more effective vaccines, higher vaccination rates, and lower poverty rates compared to Bogotá, its disease burden was significantly higher due to higher population density and, consequently, a greater number of contacts. This indicates that while more effective vaccines are crucial to flattening the curve, social distancing measures are equally important for quickly controlling the disease if the vaccination rate is not sufficiently high. Additionally, the model successfully captures the epidemiological behaviour of transmission through the use of vaccines, calculating the basic reproductive number in different scenarios and estimating the parameters of the proposed model.

***Key words*:** Basic reproductive number; COVID-19; Coronaviruses; Equilibrium; Parameter estimation; SEIVRD model; Vaccination.

Resumen

En un esfuerzo por frenar la propagación del COVID-19, se aprobaron e implementaron globalmente varios tipos de vacunas, incluidas las de ARNm, vectores virales y las tradicionales. Sin embargo, la distribución de vacunas en cada país se convirtió en un factor crítico y determinante en la evolución de la enfermedad. El presente estudio tiene como objetivo comprender el impacto diferencial de los diferentes tipos de vacunas disponibles en la carga de la enfermedad. Se propone un modelo matemático que considera múltiples vacunas en una comunidad para analizar la dinámica de transmisión del COVID-19 en dos regiones socioeconómicamente diversas. Se utilizaron datos de incidencia secundaria de las ciudades de Bogotá, Colombia, y Nueva York, EE.UU., desde marzo de 2020 hasta diciembre de 2021 para estimar los parámetros relacionados con las vacunas y las tasas reales de transmisión. Los resultados sugieren que, aunque Nueva York tiene vacunas más efectivas, mayores tasas de vacunación y menores tasas de pobreza en comparación con Bogotá, su carga de enfermedad fue significativamente mayor debido a una mayor densidad de población y, por consiguiente, un mayor número de contactos. Esto indica que, si bien las vacunas más efectivas son cruciales para aplanar la curva, las medidas de distanciamiento social son igualmente importantes para controlar rápidamente la enfermedad si la tasa de vacunación no es lo suficientemente alta. Además, el modelo captura con éxito el comportamiento epidemiológico de la transmisión mediante el uso de vacunas, calculando el número reproductivo básico en diferentes escenarios y estimando los parámetros del modelo propuesto.

***Palabras clave*:** COVID-19; Coronavirus; Equilibrio; Estimación de parámetros; Modelo SEIVRD; Número reproductivo básico; Vacunación.

1. Introduction

Coronaviruses are part of a viral family that induces mild to moderate respiratory illnesses and severe acute respiratory infections (SARI). The emergence of SARS-CoV-2, known as COVID-19, commenced in December 2019 in Hubei Province, China, and swiftly disseminated globally (Salgado et al., 2022). The development of COVID-19 vaccines was initiated in early 2020 after the identification and disclosure of the virus's genetic sequence on January 11, 2020 (Andreadakis et al., 2020). The first potential vaccine entered clinical trials on March 16, 2020 (Andreadakis et al., 2020). By April 8, 2020, there were 115 vaccine candidates, which doubled to 321 candidates by September 2020 (Andreadakis et al., 2020; Le et al., 2020). As of August 2021, 18 vaccines were approved for emergency use worldwide (Ndwandwe & Wiysonge, 2021). The primary objective of these vaccines was to prevent or mitigate the severity of COVID-19 infection.

To understand the spread of infectious diseases, compartmental models with mathematical frameworks have been employed (Brauer et al., 2012). For instance, the first deterministic epidemiological mathematical model developed to study influenza was proposed by Kermack & McKendrick (1927), utilizing systems of ordinary differential equations distinguishing three types of individuals: susceptible, infected, and recovered. Susceptible individuals are those who are likely to contract a disease upon infectious contact with infected individuals who may or may not exhibit symptoms of the disease at time t. Recovered individuals are those who are no longer infected at time t. A modified version of this model is the SIRD model, where a mortality compartment (D) at time t is also introduced, and its dynamics are studied alongside the other three compartments (Ogueda-Oliva et al., 2023). This model was utilized to describe and understand the spread of COVID-19 in Italy (Calafiore et al., 2020). It is assumed that $N = S(t) + I(t) + R(t) + D(t)$ represents the total population under study. SIRD models in mathematical epidemiology have continued to evolve, particularly for diseases classified as sexually transmitted infections such as HIV (Castillo-Chavez, 2013); vector-borne diseases such as malaria or dengue through mosquitoes (Chowell et al., 2007); both sexually and transmitted through vectors such as Zika (Padmanabhan et al., 2017); and those that can be transmitted by viruses in various ways.

On the other hand, it is imperative to grasp not only the transmission dynamics of diseases but also the ramifications of integrating effective control and mitigation strategies into modelling frameworks, which have demonstrated efficacy in reducing both contagion and mortality rates. For instance, investigations such as those by Niño-Torres et al. (2022) delve into compartmental models that encompass confinement measures, while others, exemplified by studies conducted by Yang et al. (2022), Jentsch et al. (2021), and Choi et al. (2021), incorporate the vaccination effect into their mathematical constructs. As underscored by Watson et al. (2022) and (Tchoumi et al., 2024), COVID-19 vaccination has fundamentally altered the trajectory of the pandemic. In the global effort to combat the COVID-19 pandemic, countries implemented various strategies to reduce infection transmission, including common policies like social distancing and self-quarantine. Concurrently, researchers worldwide diligently worked to develop innovative strategies to over-

come the challenges posed by this unprecedented health crisis, with vaccination emerging as a pivotal measure for disease control, offering a promising avenue to protect against infectious diseases (Khan et al., 2022).

Therefore, this work focuses on proposing a multiple vaccine compartment model, incorporating three categories of vaccines in two economically contrasting cities to a defined epidemiological model, thus evaluating its impact on COVID-19 transmission. The vaccines studied were messenger RNA vaccines, exemplified by Pfizer-BioNTech and Moderna, which showed effectiveness exceeding 90% (Katella, 2021); viral vector vaccines, such as Johnson&Johnson/Janssen and Oxford-AstraZeneca, which demonstrated effectiveness of at least 70% (Katella, 2021); and finally, traditional vaccines, like Coronavac, which achieved effectiveness of approximately 50% (BBC News, 2020). Consequently, the analysis is extended to studies such as those by Kerekes et al. (2021) or Yaladanda et al. (2022) where different vaccine types are not studied, and of Keno & Etana (2023) where vaccines are not analyzed, but rather the effect of hospitalization rate of infected people and the proportion of hospitalized patients who recover.

The variable effectiveness among different types of COVID-19 vaccines could potentially influence virus transmission, especially in regions where multiple vaccine types are implemented. The availability of vaccine varieties depends on the economic circumstances of the country or community. For example, countries with lower socioeconomic levels often relied on wealthier countries to obtain vaccines, which could affect both the quantity and quality of the vaccines received.

Motivated by these changes, a comprehensive analysis was conducted using real data from Bogotá, Colombia, obtained by the Colombian National Institute of Health (Carrillo-Larco, 2020; Ministerio de Salud y Protección Social, 2020). Additionally, data from New York, USA, provided by the Official Website of the City of New York (NYC Department of Health, 2021), were employed. In this way, the parameters of the proposed model were estimated for each city and the obtained results were compared to understand how COVID-19 transmission behaves following the inclusion of different types of vaccines.

This paper is organized as follows. Section 2 formulates our multiple vaccines model. Section 3 discusses the mathematical formulation of a model with a single vaccine and with multiple vaccines, as well as a vaccine reproduction number. In Section 4, we develop parametric estimation and numerical experiments for the cities of Bogotá and New York, and compare them. Section 5 presents our conclusions.

2. Multiple Vaccines Model

In this section, we present a multi-vaccine model to characterize the dynamics of COVID-19 transmission. We partition the model into $n+4$ compartments based on disease status as follows: Susceptible individuals denoted as S, Vaccinated individuals with vaccine type i represented as V_i (comprising n classes), Exposed individuals E, Infectious individuals I, and Recovered individuals R. Additionally,

we incorporate a compartment for deceased individuals, denoted as D, to account for fatalities resulting from COVID-19. Our model assumes that individuals who are already infected cannot receive vaccination. Moreover, once individuals recover from the infection, they acquire temporary immunity, thereby precluding subsequent reinfections. Vaccinated individuals are subject to exposure to the virus; however, they experience a reduced susceptibility compared to those without vaccination. Our investigation accounts for the imperfections inherent in vaccines, considering potential failure modes such as (i) partial effectiveness (leakiness), (ii) complete ineffectiveness (all or nothing), and (iii) waning immunity (Centers for Disease Control and Prevention, 2021*b*).

The compartment S is replenished through natural births at a rate of ΛN from the population. Individuals in the susceptible compartment can transition in two ways: they can either be vaccinated with vaccine type i and move to V_i, or they can become exposed (E), meaning they have been exposed to the pathogen but are not yet infectious or symptomatic. During the disease's incubation period, individuals in this category may be harbouring the infection and can transmit it to others, although they themselves are not contagious. Susceptible individuals transition to compartment E at a rate of $\beta SI/N$. Individuals in S are vaccinated at a rate of α, and with a probability q_i, they move to each vaccinated compartment V_i, where $q_i < 1$ and $\sum_{i=1}^{n} q_i = 1$.

Each vaccine has an efficacy κ_i, which provides protection against infection at a discounted rate of $\beta(1-\kappa_i)SI/N$ for each vaccinated compartment V_i, and they progress to the exposed class. Vaccinated individuals who have acquired long-term protection advance to the recovered class at a rate of γ_i. Exposed individuals progress to the infectious class at a rate of σ. Infected individuals recover and move to R at a constant rate of γ, or they die from the disease at a constant rate of δ and move to the deceased class, D. All compartments are subject to natural death at a rate of μ. The flow diagram for our model is shown in Figure 1.

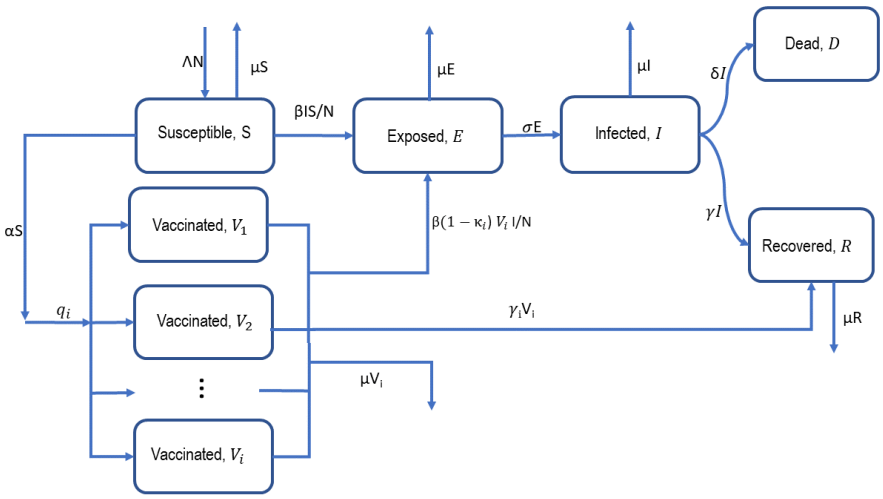

FIGURE 1: Flow diagram, $i = 1, 2, 3, \ldots, n$

The variables and parameters of the proposed model are presented in Tables 1 and 2.

Table 1: State variables for the model

Variable	Description
S	Susceptible individuals at risk of infection.
E	Exposed individuals to the pathogen but are not yet infectious or symptomatic.
I	Infected, infected individuals who are infectious.
V_i	Vaccinated, individuals who are fully vaccinated with vaccine i.
R	Recovered, individuals who have recovered from the virus.
D	Deceased, individuals who died due to COVID-19 infection.

Table 2: Parameters for the model

Parameter	Description
Λ	Natural birth rate.
β	Transmission rate of COVID-19.
κ_i	Efficacy in preventing COVID-19 infection of vaccine i.
α	Overall rate of vaccination.
q_i	proportion vaccinated with vaccine i.
σ	Fraction of exposed individuals moving to infected.
γ	Recovery rate.
γ_i	Recovery rate of individuals vaccinated with vaccine i.
δ	Death rate due to COVID-19.
μ	Natural death rate.

Our deterministic model equations are as follows:

$$\begin{aligned}
\frac{dS}{dt} &= \Lambda N - \beta\frac{SI}{N} - (\mu+\alpha)S,\\
\frac{dE}{dt} &= \beta\frac{SI}{N} + \beta\frac{I}{N}\sum_{i=1}^{n}(1-\kappa_i)V_i - (\sigma+\mu)E,\\
\frac{dV_i}{dt} &= \alpha q_i S - \beta(1-\kappa_i)\frac{V_i I}{N} - (\gamma_i+\mu)V_i,\\
\frac{dI}{dt} &= \sigma E - (\gamma+\delta)I - \mu I,\\
\frac{dR}{dt} &= \gamma I + \sum_{i=1}^{n}\gamma_i V_i - \mu R,\\
\frac{dD}{dt} &= \delta I.
\end{aligned} \tag{1}$$

where $N = S + \sum_{i=1}^{n} V_i + E + I + R$ for $i = 1, 2, 3, \ldots, n$.

3. Mathematical Analysis

This section aims to develop the proposed model in (1) mathematically. Firstly, we will establish the non-negativity and boundedness of the model solutions. It is noteworthy that the demonstration of the existence and uniqueness of solutions in epidemiological models has been extensively addressed in Sadri et al. (2023) and Yoshida (2023). Therefore, our focus in this section will be on elucidating the endemic equilibrium and basic reproduction number. We conduct analyses on three sub-models: (i) multiple vaccine model, (ii) two-vaccine model, and (iii) single vaccine model.

Theorem 1. *Let the initial conditions* $\{S(0), E(0), V_i(0), I(0), R(0), D(0)\} > 0$. *Then the solutions to the system (1) are non-negative in* $[0, \infty]$.

Proof. All right hand side terms of the system (1) are continuous and locally Lipschitz on $\mathbb{R}$.

The solution $\{S(t), E(t), V_i(0), I(0), R(0), D(0)\}$ with their initial conditions exist and are unique in the interval $[0, \infty)$ (Martcheva, 2015).

From the first equation in (1), we obtain

$$\frac{dS}{dt} = \Lambda N - (G(t) + \eta)S,$$

where $G(t) = \beta \dfrac{I}{N}$ and $\eta = \mu + \alpha$. This equation can be rewritten as,

$$\frac{d}{dt}\left[S(t)\, e^{\, f(t)}\right] = \Lambda N e^{\, f(t)},$$

for $f(t) = \eta t + \displaystyle\int_0^t G(\tau) d\tau$.

Integrating both sides of the above relation with respect to t, we obtain

$$S(t_1)\, e^{\, f(t_1)} - S(0) = \Lambda N \int_0^{t_1} e^{\, f(x)} dx.$$

Since $S(0) \geq 0$, we have,

$$S(t_1)\, e^{\, f(t_1)} \geq \Lambda N \int_0^{t_1} e^{\, f(x)} dx,$$

which yields,

$$S(t_1) \geq e^{-f(t_1)} \Lambda N \int_0^{t_1} e^{\, f(x)} dx > 0.$$

This proves that $S(t) > 0$. Similarly, we can show $E(t) > 0, V_i(t) > 0, I(t) > 0, R(t) > 0$ and $D(t) > 0$ starting with the respective equations in (1), which completes the proof. □

3.1. Basic Reproductive Number

The basic reproductive number $\mathcal{R}_0$ is the expected number of cases directly generated by an infected individual in a population, assuming no other individuals are infected or immunized. In our model, we have an exposed population, E, and an infected population, I. Hence, we take $m = 2$. We will employ two different methods to calculate $\mathcal{R}_0$: the endemic equilibrium method and the next-generation matrix method.

Let F and V be defined as follows,

$$\begin{aligned} F &= \begin{bmatrix} 0 & \frac{\Lambda\beta}{\mu+\alpha} + \frac{\Lambda\beta}{\mu+\alpha}\sum_{i=1}^{n}(1-\kappa_i)\frac{\alpha q_i}{\gamma_i+\mu} \\ 0 & 0 \end{bmatrix}, \\ V &= \begin{bmatrix} \sigma+\mu & 0 \\ -\sigma & \gamma+\delta+\mu \end{bmatrix}, \\ FV^{-1} &= \begin{bmatrix} n_{11} & n_{12} \\ 0 & 0 \end{bmatrix}, \end{aligned}$$

where,

$$n_{11} = \frac{\sigma\frac{\Lambda\beta}{\mu+\alpha}\left(1+\sum_{i=1}^{n}(1-\kappa_i)\frac{\alpha q_i}{\gamma_i+\mu}\right)}{(\sigma+\mu)(\gamma+\delta+\mu)},$$

and,

$$n_{12} = \frac{\frac{\Lambda\beta}{\mu+\alpha}\left(1+\sum_{i=1}^{n}(1-\kappa_i)\frac{\alpha q_i}{\gamma_i+\mu}\right)}{\gamma+\delta+\mu}.$$

The reproduction number is defined as the dominant eigenvalue of FV^{-1}, expressed as:

$$\mathcal{R}_{0v}^{n} = \mathcal{R}_0 + \mathcal{R}_{vn}. \tag{2}$$

The threshold parameter,

$$\mathcal{R}_{vn} = \sum_{i=1}^{n}\left(\frac{\Lambda(1-\kappa_i)}{\mu+\alpha}\right)\left(\frac{\alpha q_i}{\gamma_i+\mu}\right)\mathcal{R}_0,$$

is the control reproduction number for n vaccine types, while

$$\mathcal{R}_0 = \frac{\sigma\beta}{(\sigma+\mu)(\gamma+\delta+\mu)},$$

is the basic reproduction number in the absence of intervention. Therefore, the inclusion of vaccines with their respective parameter ($\kappa_i \to 1$) has a high potential to contain the outbreak of the disease.

3.2. Multiple Vaccine Model

The first model we are interested in is the general model for $i = 1, 2, 3, \ldots, n$ number of vaccines. In this problem, we focus on the determination of the disease-free equilibrium and the basic reproduction number of the model, as will be seen below. Setting each equation of model (1) to 0, we get:

$$\begin{aligned}
\Lambda N - \alpha S^* - \beta \frac{S^* I^*}{N} - \mu S^* &= 0, \\
\beta \frac{S^* I^*}{N} + \beta \frac{I^*}{N} \sum_{i=1}^{n} (1-\kappa_i) V_i^* - (\sigma + \mu) E^* &= 0, \\
\alpha q_i S^* - \beta (1-\kappa_i) \frac{V_i^* I^*}{N} - (\gamma_i + \mu) V_i^* &= 0, \\
\sigma E^* - (\mu + \gamma + \delta) I^* &= 0, \\
\gamma I^* + \sum_{i=1}^{n} \gamma_i V_i^* - \mu R^* &= 0.
\end{aligned}$$

Substituting for E^* in the second equation, we obtain,

$$I^* = 0 \text{ or } N^* = \mathcal{R}_0 \left[S^* + \sum_{i=1}^{n} (1-\kappa_i) V_i^* \right]$$

where,

$$\mathcal{R}_0 = \frac{\sigma \beta}{(\mu + \sigma)(\mu + \gamma + \delta)}, \tag{3}$$

is the basic reproduction number.

Note that,

$$\mathcal{R}_0 = \frac{1}{x_v^*}$$

where

$$x_v^* = S^*/N^* + \sum_{i=1}^{n} (1-\kappa_i) V_i^*/N^*$$

is the standard fraction of the hosts who are susceptible and vaccinated at equilibrium.

The solution $I^* = 0$ leads to,

$$E^* = R^* = 0,$$

and,

$$\tilde{S} = \frac{\Lambda N^*}{\mu + \alpha}, \text{ and, } V_i^* = \frac{\alpha q_i}{\gamma_i + \mu} \tilde{S} = \frac{\alpha q_i \Lambda N^*}{(\gamma_i + \mu)(\mu + \alpha)},$$

for $i = 1, 2, \ldots, n$. Thus, the disease-free equilibrium is given by,

$$DFE = \left(\tilde{S}, \frac{\alpha q_1 \tilde{S}}{(\gamma_1 + \mu)}, \frac{\alpha q_2 \tilde{S}}{(\gamma_2 + \mu)}, \ldots, \frac{\alpha q_n \tilde{S}}{(\gamma_n + \mu)}, 0, 0, 0 \right).$$

Thus, the solution is

$$N^* = \mathcal{R}_0 \left[S^* + \sum_{i=1}^{n} (1-\kappa_i) V_i^* \right].$$

3.3. Two Vaccines Model

The disease-free equilibrium for a two-vaccine compartmental model is given by,

$$DFE = \left(\tilde{S},\ \frac{\alpha q_1 \tilde{S}}{(\gamma_1 + \mu)}, \frac{\alpha q_2 \tilde{S}}{(\gamma_2 + \mu)},\ 0,\ 0,\ 0 \right),$$

where $\tilde{S} = \dfrac{\Lambda N^*}{\mu + \alpha}$. The endemic equilibrium points are obtained by solving the system of equations,

$$\begin{aligned}
S^* &= \frac{\Lambda N^*}{\mu + \alpha + B^*}, \\
V_1^* &= \left(\frac{\alpha q_1}{\gamma_1 + \mu + (1-\kappa_1) B^*} \right) \left(\frac{\Lambda N^*}{\mu + \alpha + B^*} \right), \\
V_2^* &= \left(\frac{\alpha q_2}{\gamma_2 + \mu + (1-\kappa_2) B^*} \right) \left(\frac{\Lambda N^*}{\mu + \alpha + B^*} \right), \\
N^* &= \mathcal{R}_0 [S^* + (1-\kappa_1) V_1^* + (1-\kappa_2) V_2^*],
\end{aligned}$$

in terms of B^*. So substituting for S^*, V_1^* and V_2^* in the equation for N, we obtain,

$$N^* = \mathcal{R}_0 \left(\frac{\Lambda N^*}{\mu + \alpha + B^*} \right) [1 + v_1 + v_2],$$

where,

$$\begin{aligned}
v_1 &= \frac{\alpha q_1 (1-\kappa_1)}{\gamma_1 + \mu + (1-\kappa_1) B^*}, \\
v_2 &= \frac{\alpha q_2 (1-\kappa_2)}{\gamma_2 + \mu + (1-\kappa_2) B^*},
\end{aligned}$$

which yields a trivial solution

$$N^* = 0,$$

which is not biologically useful. Conditions for the existence of endemic equilibrium point(s) are determined from analysis of the coefficients of the cubic equation,

$$m_3 {B^*}^3 + m_2 {B^*}^2 + m_1 B^* + m_0 = 0, \tag{4}$$

where,

$$\begin{aligned} m_3 &= (1-\kappa_1)(1-\kappa_2), \\ m_2 &= \Lambda(1-\kappa_1)(1-\kappa_2)(\psi_{2c}-\mathcal{R}_0), \\ m_1 &= \{\Lambda[(\mu+\mu_1)(1-\kappa_2)+(\mu+\mu_2)(1-\kappa_1)]+ \\ &\quad \alpha(1-\kappa_1)(1-\kappa_2)]\}(\psi_{3c}-\mathcal{R}_0), \\ m_0 &= (\mu+\alpha)(\mu+\gamma_1)(\mu+\gamma_2)(1-\mathcal{R}_{0v}^2), \end{aligned}$$

with,

$$\begin{aligned} \psi_{2c} &= \frac{\mu+\gamma}{\Lambda}+\frac{\mu+\gamma_1}{\Lambda(1-\kappa_1)}+\frac{\mu+\gamma_2}{\Lambda(1-\kappa_2)}, \\ \psi_{3c} &= \frac{(\mu+\gamma_1)(\mu+\gamma_2)+(\mu+\alpha)\Theta}{\Lambda\Theta+\alpha(1-\kappa_1)(1-\kappa_2)]}, \\ \Theta &= [(\mu+\mu_1)(1-\kappa_2)+(\mu+\mu_2)(1-\kappa_1)] \end{aligned}$$

and,

$$\mathcal{R}_{0v}^2 = \frac{\Lambda\mathcal{R}_0}{\mu+\alpha}\left(1+\frac{\alpha q_1(1-\kappa_1)}{\mu+\gamma_1}+\frac{\alpha q_2(1-\kappa_2)}{\mu+\gamma_2}\right).$$

3.4. Single Vaccine Model

Setting each model equation to zero and,

$$B=\beta\left(\frac{I}{N}\right),$$

we get the following:

$$\begin{aligned} \Lambda N^*-\alpha S^*-B^*S^*-\mu S^* &= 0, \\ B^*S^*+(1-\kappa)B^*V^*-(\mu+\sigma)E^* &= 0, \\ \alpha qS^*-(1-\kappa)B^*V^*-(\mu+\gamma_1)V^* &= 0, \\ \sigma E^*-(\mu+\gamma+\delta)I^* &= 0, \\ \gamma I^*+\gamma_1 V^*-\mu R^* &= 0, \end{aligned}$$

with state solutions,

$$\begin{aligned}
S^* &= \frac{\Lambda N^*}{\mu+\alpha+B^*},\\
E^* &= \left(\frac{S^*+(1-\kappa)V^*}{\mu+\sigma}\right)B^*,\\
V^* &= \frac{\alpha q S^*}{\mu+\gamma_1+(1-\kappa)B^*},\\
&= \left(\frac{\alpha q}{\mu+\gamma_1+(1-\kappa)B^*}\right)\left(\frac{\Lambda N^*}{\mu+\alpha+B^*}\right),\\
I^* &= \left(\frac{\sigma}{\mu+\gamma+\delta}\right)E^* = \left(\frac{\sigma}{\mu+\gamma+\delta}\right)\left(\frac{S^*+(1-\kappa)V^*}{\mu+\sigma}\right)B^*,\\
R^* &= \frac{\gamma I^*+\gamma_1 V^*}{\mu},
\end{aligned}$$

By substituting for I^* in the equation for B, we obtain:

$$B^* = 0 \text{ or } N^* = \mathcal{R}_0[S^*+(1-\kappa)V^*]$$

where $\mathcal{R}_0$ is defined as in Equation (3). The solution $B^* = 0$ leads to the disease-free equilibrium given by,

$$DFE = \left(\frac{\Lambda N^*}{\mu+\alpha},\ \frac{\alpha q \Lambda N^*}{(\gamma_1+\mu)(\mu+\alpha)},\ 0,\ 0,\ 0\right).$$

The solution $N^* = \mathcal{R}_0[S^*+(1-\kappa)V^*]$ together with system of equations,

$$\begin{aligned}
S^* &= \frac{\Lambda N^*}{\mu+\alpha+B^*} \text{ and}\\
V^* &= \left(\frac{\alpha q}{\gamma_1+\mu+(1-\kappa)B^*}\right)\left(\frac{\Lambda N^*}{\mu+\alpha+B^*}\right),
\end{aligned} \tag{5}$$

lead to,

$$N^* = 0,$$

a trivial solution that is not biologically useful or endemic equilibrium from analysing the roots of the quadratic equation,

$$m_2 B^{*2} + m_1 B^* + m_0 = 0, \tag{6}$$

where,

$$\begin{aligned}
m_2 &= 1-\kappa,\\
m_1 &= \Lambda(1-\kappa)(\psi_{1c}-\mathcal{R}_0),\\
m_0 &= \mu(\mu+\alpha)(1-\mathcal{R}^1_{0v}).
\end{aligned} \tag{7}$$

Where,

$$\psi_{1c} = \left(\frac{\mu+\gamma}{\Lambda}\right)\left(1+\frac{\mu+\gamma_1}{(\mu+\gamma)(1-\kappa)}\right) \text{ and,}$$

$$\mathcal{R}^1_{0v} = \left(\frac{\Lambda}{\mu+\alpha}\right)\left(1+\left(\frac{\alpha}{\gamma_1+\mu}\right)q(1-\kappa)\right)\mathcal{R}_0.$$

The solutions of the quadratic equation are,

$$B^* = \frac{-m_1 \pm \sqrt{m_1^2 - 4m_2 m_0}}{2m_2},$$

where $m_i s$ are as presented in (7). Clearly,

1. If $\psi_{1c} < \mathcal{R}_0$ and $\mathcal{R}_{0v}^1 < 1$, B^* has two distinct positive real roots.
2. If $\psi_{1c} < \mathcal{R}_0$ and $\mathcal{R}_{0v}^1 > 1$, B^* has two distinct real roots of opposite signs.
3. If $\psi_{1c} < \mathcal{R}_0$ and $\mathcal{R}_{0v}^1 = 1$, B^* has roots $B_-^* = 0$ and $B_+^* = R - \psi_{1c} > 0$.
4. If $\psi_{1c} > \mathcal{R}_0$ and $\mathcal{R}_{0v}^1 < 1$, B^* has two distinct negative real roots.
5. If $\psi_{1c} > \mathcal{R}_0$ and $\mathcal{R}_{0v}^1 > 1$, B^* has two distinct real roots of opposite signs.
6. If $\psi_{1c} > \mathcal{R}_0$ and $\mathcal{R}_{0v}^1 = 1$, B^* has roots $B_-^* = 0$ and $B_+^* = -(\psi_{1c} - \mathcal{R}_0) < 0$.

The results can be succinctly summarized by the following theorem,

Theorem 2. *Consider system (1), with one vaccine*

1. *If $\psi_{1c} < \mathcal{R}_0$ and $\mathcal{R}_{0v}^1 < 1$ there exist two distinct endemic equilibrium given $B^* = B_-^*(\cdot)$ and $B^* = B_-^*(\cdot)$.*
2. *If $\psi_{1c} < \mathcal{R}_0$ and $R_{0v}^1 \geq 1$ there a unique endemic equilibrium point given $B^* = B_-^*(\cdot)$.*
3. *If $\psi_{1c} > \mathcal{R}_0$ and $\mathcal{R}_{0v}^1 \leq 1$, there are endemic equilibrium points. Thus only the disease-free equilibrium exists.*

4. Analysis and Discussions

In this section, we present the development of the model, analyzing the dynamics of COVID-19 disease with vaccination in two cities with different socioeconomic characteristics: Bogotá, Colombia, and New York, USA. To assess the performance of the deterministic model, we used real data to estimate the parameters, conduct numerical simulations, and subsequently discuss the results.

First, we will outline the method used to estimate the model parameters, employing real data provided by the available database of the National Institute of Health of Colombia (INS) (Carrillo-Larco, 2020; Ministerio de Salud y Protección Social, 2020) and the Official Website of the City of New York (NYC Department of Health, 2021). These data sources provide daily numbers of cases for both infected individuals and reports of recovered and deceased persons. Additionally, we have taken into account the number of vaccinated individuals in both cities. We estimated parameters to conduct numerical simulations of the deterministic models. Subsequently, we compared the results of the two models and their accuracy with the data (Rosenberg et al., 2022; Tchoumi et al., 2024).

4.1. Parametric Estimation

Herein, we outline the methodology employed to estimate the parameters of the epidemiological model (1). This approach relies on ordinary least squares (OLS) analysis to scrutinize the alignment between model outcomes and the gathered dataset. Such an approach has demonstrated efficacy in parameter estimation, as evidenced by previous studies such as Wang et al. (2022), Khan et al. (2014), and Cintrón-Arias et al. (2008).

We define the vector of parameters to be estimated, represented by $\theta = (\kappa, \alpha, q, \gamma_1)$. Estimates of the vector θ will be obtained by minimizing the difference between the observed values and the values predicted by the model (1) at each time point. It is important to specify that, given the data conditions, the values for $\Lambda, \sigma, \gamma, \delta$, and μ were kept fixed for both cities based on available literature.

It is emphasized that initial conditions for the parameters are included. In our context, θ_0 represents the parameter vector containing the true values. The n analyzed observations are denoted by Y_j. Moreover,

$$Y_j = z(t_j; \theta_0) + \epsilon_j \quad \text{for} \quad j = 1, \ldots, n, \tag{8}$$

where $z(t_j; \theta_0)$ denotes the incidence estimated by the model using the initial conditions provided in θ_0 and the errors, ϵ_j, are assumed to be independent and identically distributed random variables with zero mean. This assertion is supported by Cintrón-Arias et al. (2008). Thus, we denote our set of observations as $Y = (Y_1, \ldots, Y_n)$, and define the estimator θ_{OLS} as follows,

$$\theta_{OLS}(Y) = \theta_{OLS}^n(Y) = \underset{\theta \in \Theta}{\operatorname{argmin}} \sum_{j=1}^{n} \left[Y_j - z(t_j; \theta_0) \right]^2. \tag{9}$$

Here, Θ represents the parameter space where the estimations of θ reside. Therefore, once we have defined the objective function to minimize (9), we proceed to utilize the Nelder-Mead optimization algorithm to adjust the parameters of the model (1) in order to minimize said objective function. This method is suitable for addressing nonlinear optimization problems and does not require gradient calculations (Calleri et al., 2021). The algorithm adjusts the parameters through iterations in the direction that decreases the objective function. During each iteration, we calculate the predicted values for each time point using the equations of the model (1) and the current parameter values. Once the optimization process is completed, the estimated parameter values of the model (1) represent the optimal estimations that minimize the discrepancy between the observed and predicted values in the dataset.

Particularly, we use *Nelder-Mead* in the minimize function of SciPy (Virtanen et al., 2020), an open-source software library based on Python (Van Rossum & Drake, 2009).

4.2. Bogotá City, Colombia

In our study, we initially gathered data from Bogotá, Colombia, to estimate the parameters for our model. The first recorded case of COVID-19 infection in Bogotá occurred in early March 2020. Since then, the country has documented nearly 5 million confirmed cases and 127 thousand deaths (World Health Organization, 2021). Vaccination efforts commenced in Colombia in February 2021, with the approval of five vaccines for administration: Pfizer-BioNTech, Moderna, J&J/Janssen, AstraZeneca, and CoronaVac (COVID19 Vaccine Tracker, 2021). As of now, almost 20 million people have been fully vaccinated. Following the onset of vaccination, a third wave of infections occurred. The data specific to Bogotá was sourced from the National Institute of Health, covering the period from March 6, 2020, to August 30, 2021 (National Institute of Health, 2021; Niño-Torres et al., 2021). Table 3 provides a summary of the data for Bogotá, while Figures 2(a), 2(b), and 2(c) offer both numerical and visual representations of the provided data. The statistics on recovered, susceptible, and deceased individuals are depicted as proportions of the total population of Bogotá, which stands at 7 181 million people.

Table 3: Summary statistics for data in Bogotá, Colombia

	Day	Infected	Dead	Recovered	Susceptible
Min	7	4	0	0.00000013	0.7423
1st Qu	147.5	886.5	3164	0.005995	0.8376
Median	279	1.916	8936	0.04495	0.8809
Mean	278.8	2733.2	10645	0.05954	0.8660
3rd Qu	410.5	3871	15243	0.08716	0.9205
Max	542	15570	27428	0.1814	0.9273

In Table (4), we have set fixed values for Λ, β, σ, γ, δ, and μ, and conducted parameter estimation for κ, α, q, and γ_1, as these pertain to vaccine-related factors. The fixed parameter values are sourced from various references (as indicated in the table above). Due to data availability, Λ, γ, δ, and μ pertain to Colombia rather than specifically to Bogotá. As per our parameter definitions (refer to the Table of Parameters), Λ denotes the natural birth rate. We have estimated β to be the transmission rate of COVID-19, set at 0.8. We assign $\sigma = 1/6$ to represent the incubation period, which is estimated to be 6 days; γ stands for the recovery rate of COVID-19, while δ indicates the mortality rate due to the disease. Lastly, μ represents the natural death rate. To determine these essential parameters, we employ the methodology outlined in Subsection 4.1.

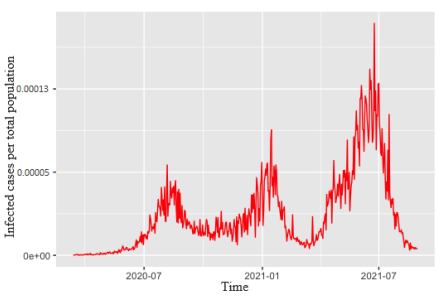

(a) Active infected cases in Bogotá, Colombia from March 6, 2020, to August 2021

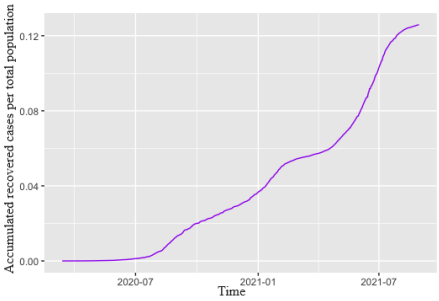

(b) Recovered cases in Bogotá, Colombia from March 6, 2020, to August 2021

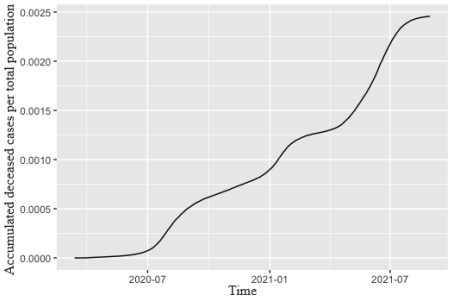

(c) Deceased cases in Bogotá, Colombia from March 6, 2020, to August 2021

FIGURE 2: Numerical and visual representation of the provided data of Bogotá City, Colombia

TABLE 4: Parameter estimation for Bogotá, Colombia

Parameter	Value	Source
Λ	0.01651	Central Intelligence Agency (2021)
β	0.8	Estimated
κ	0.99	Estimated
α	0.01183	Estimated
q	0.0016	Estimated
σ	0.167	CDC (2020)
γ	0.969	CoronaTracker (2021)
γ_1	0.0007	Estimated
δ	0.0255	Reuters (2021*a*)
μ	0.00553	Central Intelligence Agency (2021)

The estimated parameters are now utilized to simulate outcomes for Bogotá, Colombia. In Figures 3, 4, 5, and 6, each graph features the actual data depicted by the purple line, while the model simulation results are represented by the blue line. A vertical indicator line is present on each graph to denote significant events; the yellow dashed line marks the commencement of vaccination efforts. The four simulations presented below encompass accumulated infected cases, active infected cases, recovered cases, and deceased cases. Each simulation spans the same 200-day time frame.

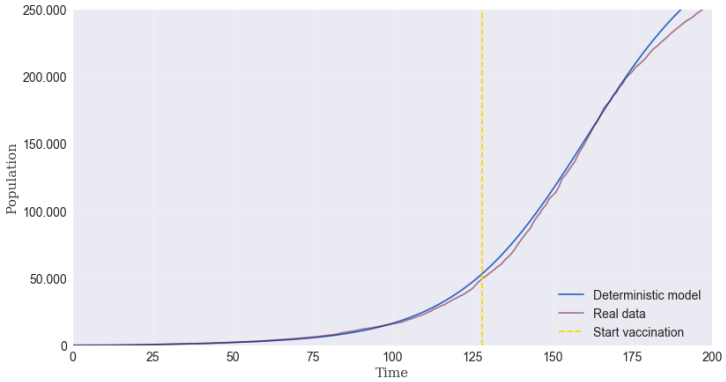

FIGURE 3: Comparison of simulated and actual accumulated infected cases in Bogotá, Colombia

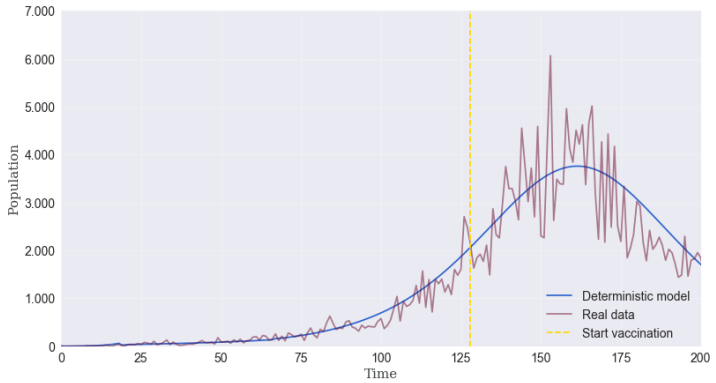

FIGURE 4: Comparison of simulated and actual active infected cases in Bogotá, Colombia

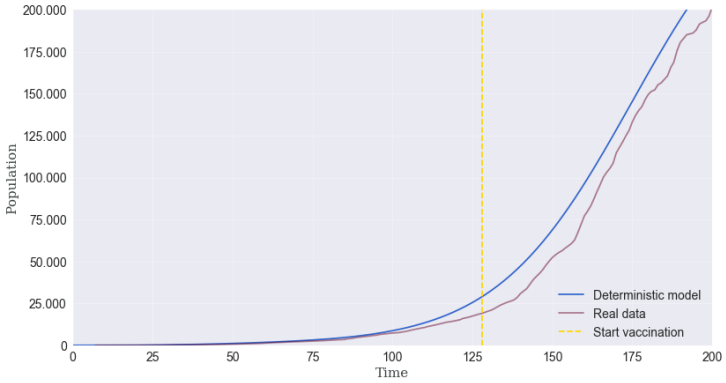

FIGURE 5: Comparison of simulated and actual recovered cases in Bogotá, Colombia

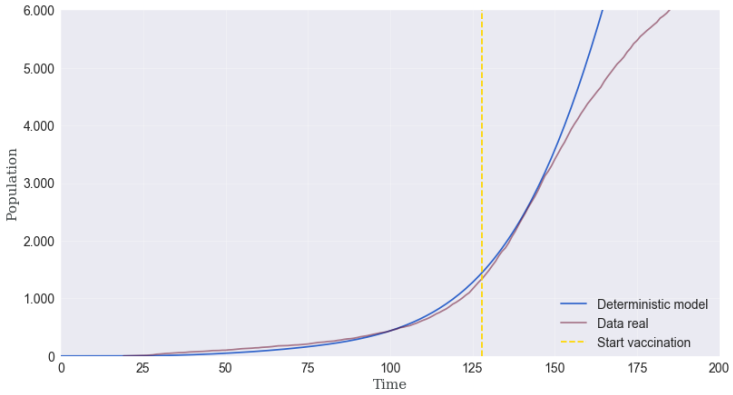

FIGURE 6: Comparison of simulated and actual deceased Cases in Bogotá, Colombia

4.3. New York City, NYC, USA

Based on information retrieved from the Official Website of the City of New York (NYC Department of Health, 2022*b*), the initial case of COVID-19 infection in NYC was reported on February 29, 2020 (Zhang et al., 2021). Subsequently, the city encountered three waves of infections in April 2020, January 2021, and January 2022, respectively. COVID-19 vaccination efforts in NYC commenced in December 2020, with vaccines developed by Pfizer, Moderna, AstraZeneca, and Janssen being approved. By January 2021, approximately 75% of the population had been fully vaccinated (excluding booster shots) (NYC Department of Health, 2022*a*). Data collection for COVID-19 cases in NYC for this study commenced on July 7, 2021, and concluded on October 5, 2021 (NYC Department of Health, 2021). In Table 5 are written summary statistics, numerical analyses, and graphical simulations derived from the collected data for NYC. Active infections, recoveries, and deceased are presented as proportions relative to the total population of 8.82 million individuals.

TABLE 5: Summary statistics for data in NYC, USA

	Day	Infected	Dead	Recovered	Susceptible
Min	1	236	1	0.1094	0.7734
1st Qu	23.5	867.5	5	0.1118	0.8035
Median	46	1196	9	0.1120	0.8359
Mean	46	1169.2	8.7	0.1119	0.8325
3rd Qu	68.5	1568	12.5	0.1123	0.8604
Max	91	1927	20	0.1126	0.88897

It can be observed from Figure 7(a) that the count of active infected cases in NYC fluctuates between July 7, 2021, and October 5, 2021, the period for which the data was collected. Overall, the count of active infected cases experienced rapid growth from July to mid-August, followed by a gradual decline thereafter. Figure 7(b) depicts the count of recovered cases in NYC. The plot illustrates a

sharp increase in the count of recovered cases from July 7 to early August, followed by a continuing but slower rate of increase. Regarding deceased cases as illustrated in Figure 7(c), the count is observed to rise from July 7, 2021, to September 10, 2021, with a subsequent decrease in cases thereafter.

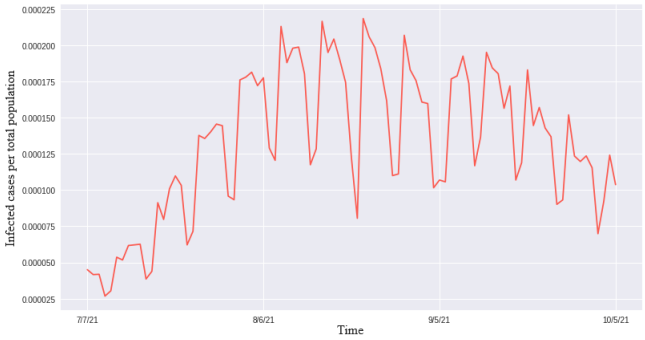

(a) Active infected cases in New York City, NYC, USA since July 7, 2021

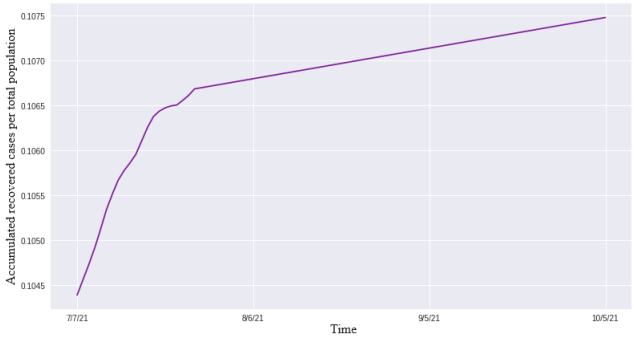

(b) Recovered cases in New York City, NYC, USA since July 7, 2021

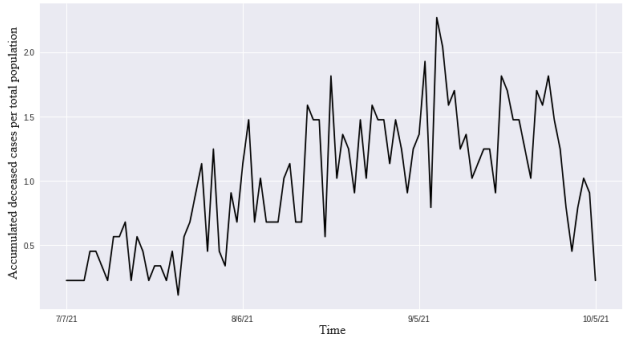

(c) Deceased cases in New York City, NYC, USA since July 7, 2021

FIGURE 7:

In Table 6, we present the parameter estimations for New York City, where we have fixed the values of the following parameters: Λ, β, σ, γ, δ, and μ. Similar to the parameter estimation process for Bogotá, Colombia, only the parameters associated with vaccination were estimated, including κ, α, q, and γ_i.

Table 6: Parameter estimation for NYC, USA

Parameter	Estimated Value	Source
Λ	0.0572	Centers for Disease Control and Prevention (2021*a*)
β	0.91	Statista (2021)
κ	0.72112	Estimated
α	0.66195	Estimated
q	0.6899	Estimated
σ	0.069	Our World in Data (2021)
γ	0.76	Silver (2021)
γ_1	0.05247	Estimated
δ	0.0308	Google News (2021)
μ	0.0572	Centers for Disease Control and Prevention (2021*a*)

These estimated parameters are then utilized to simulate outcomes for New York City, NY, USA. As observed in the simulations for Bogotá, each graph displays the actual data represented by the purple line and the model simulation results depicted by the blue line. A vertical indicator line is included in each graph to mark significant events, such as the initiation of vaccination, denoted by the yellow dashed line. The four simulations presented encompass accumulated infected cases, active infected cases, recovered cases, and deceased cases, each covering a time frame of 100 days.

Figures 8 to 11 showcase the graphical results of the numerical simulations for NYC. While the simulation results demonstrate overall accuracy, some discrepancies are evident in the graphs. Notably, the estimation for accumulated infected cases in NYC, as illustrated in Figure 8, closely aligns with the real data. Similarly, the estimation for active infected cases in NYC, as depicted in Figure 9, is reasonably accurate, albeit capturing only a few variations in the real data. Regarding recovered and deceased cases, both simulations effectively capture the trends observed in the real data; however, they slightly underestimate the actual figures, as evidenced by Figures 10 and 11.

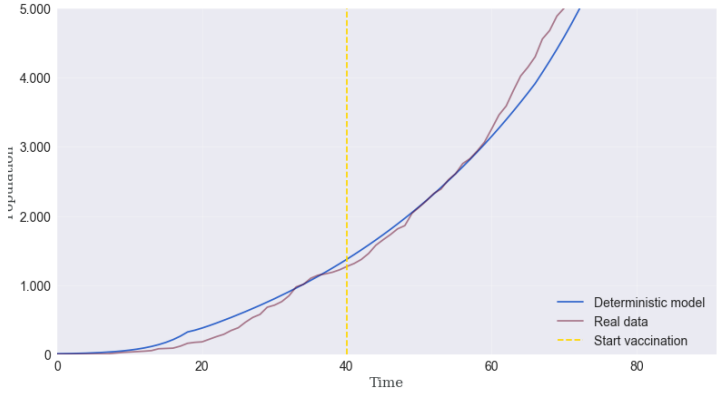

FIGURE 8: Comparison of simulated and actual accumulated infected cases in New York City, NYC, USA

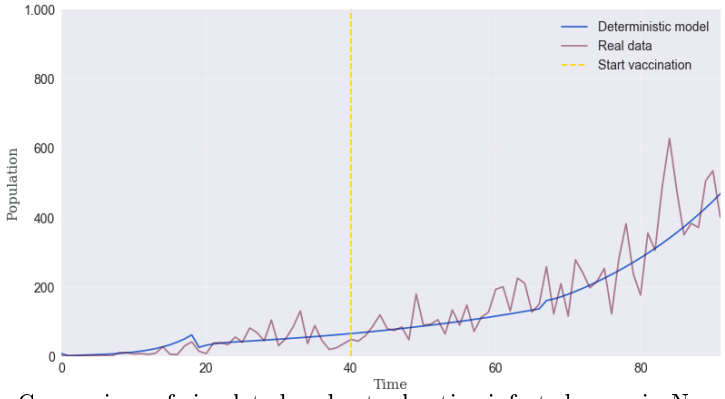

FIGURE 9: Comparison of simulated and actual active infected cases in New York City, NYC, USA

4.4. Comparison Between Two Cities

In Table 7, we present a comparative analysis of the outcomes observed in the cities of Bogotá and New York City. The table below juxtaposes key parameter values, as estimated by our model, pertaining to vaccination and the transmission dynamics of COVID-19. To facilitate a comprehensive comparison between Bogotá and New York City, we focus on evaluating the values of β (infection rate), κ (vaccine efficacy), α (vaccination rate), and γ_1 (recovery rate for vaccinated individuals). These parameters serve as pivotal indicators to delineate the disparities in outcomes between the two cities and to offer initial insights into our research inquiry. The respective values of these parameters for both cities are presented, along with the percentage difference observed between them. Additionally, the table includes abbreviations such as P.D. for Population Density and P.R. for Poverty Rate.

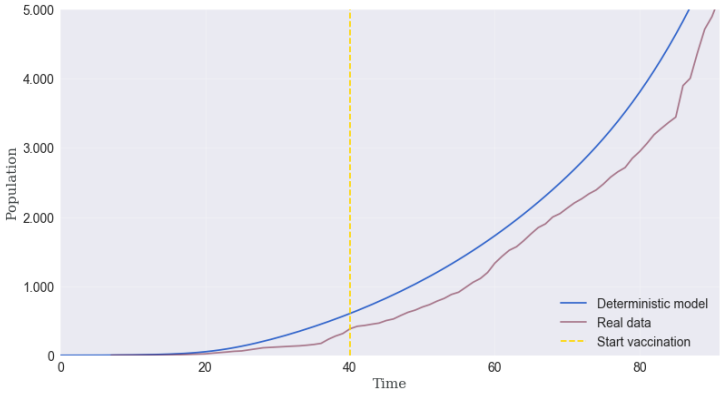

FIGURE 10: Comparison of simulated and actual recovered cases in New York City, NYC, USA

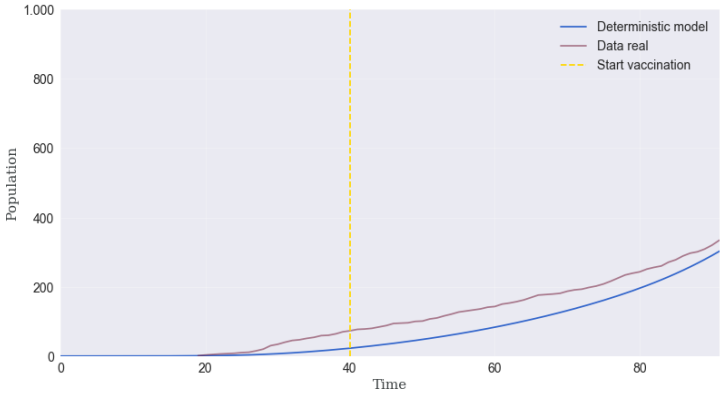

FIGURE 11: Comparison of simulated and actual deceased Cases in New York City, NYC, USA

TABLE 7: Percentage difference of selected parameters

Parameter	Bogotá	New York City	% Difference
Transmission rate (β)	0.8	0.91	13%
Vaccine efficacy (κ)	0.99	0.72112	27%
Vaccination rate (α)	0.01183	0.66195	5496%
Recovery rate of vaccinated (γ_1)	0.0007	0.05247	7396%
Population Density (P.D.)	18,000/mi^2	27,000/mi^2	50%
Poverty Rate (P.R.)	29.4%	13.4%	54.4%

In 2019, the poverty rate in the United States stood at 13.4% (DePietro, 2021). In Colombia, the poverty rate for the same year was recorded at 29.40%, with a subsequent increase to an estimated 37.5% by the conclusion of 2020 (Macrotrends, 2019; Reuters, 2021*b*). The United States primarily administers mRNA vaccines, such as Pfizer-BioNTech and Moderna. In contrast, Colombia's vaccine distribution includes a combination of mRNA vaccines, including Pfizer-BioNTech and Moderna, as well as viral vector or traditional vaccines like Sinovac, Oxford-

AstraZeneca, and J&J/Janssen. Notably, the majority of vaccines administered in Colombia are Sinovac, a traditional inactivated virus vaccine manufactured in China (Unidad de salud, 2021). Colombia relies heavily on importing vaccines from other nations, resulting in a more limited supply compared to the United States.

At the commencement of the data collection period for Bogotá, vaccination had not yet commenced. By the end of this period, the proportion of vaccinated individuals reached 0.289 or 28.9% (Our World in Data Colombia, 2021). Conversely, at the onset of the data collection period for New York City, approximately 54.8% of the population had received vaccinations, increasing to 64.3% by the conclusion of the study period (Our World in Data USA, 2021). While the transmission rate, denoted by β, is 13.5% higher in New York City, the city exhibits a 27% greater vaccine efficacy and significantly higher rates of overall vaccination compared to Bogotá, as indicated by estimates from the deterministic model. This variance can be attributed to socioeconomic disparities, with vaccines being more readily available in New York City. The increased vaccine efficacy observed in New York City may be attributed to the types of vaccines accessible there in contrast to those available in Bogotá. Additionally, New York City's population density exceeds 27 000 individuals per square mile, surpassing Bogota's density of approximately 18 000 individuals per square mile (NYC Department of City Planning, 2022; World's Capital Cities, 2022). This disparity in population density could contribute to the heightened transmission rate observed in New York City.

5. Concluding Remarks

In this study, we investigate the efficacy of vaccines in combating the COVID-19 pandemic, utilizing real data from two socioeconomically diverse cities, Bogotá D.C. and New York City. Initially, we develop a deterministic model incorporating multiple vaccine compartments to elucidate the dynamics of COVID-19 transmission and calculate the basic reproductive number in different scenarios. Subsequently, we conduct mathematical analyses to gain insights into the implementation of various vaccine types in these two cities. We perform parameter estimations and numerical simulations to assess the validity of our deterministic models. Our findings, supported by numerical and graphical evidence, affirm the suitability of our model for the observed data from these divergent urban landscapes. Furthermore, we compare the vaccine-related parameters inferred from our models to elucidate the influence of socioeconomic disparities on vaccination strategies between the two cities.

In future endeavours, we aim to expand parametric estimation and numerical simulations by incorporating methodologies that involve neural networks, such as Disease Informed Neural Networks proposed in Ogueda-Oliva et al. (2023). This will enable us to compare the estimations conducted thus far and those derived from novel approaches.

Additionally, we propose extending our model validation to encompass data from cities across countries exhibiting diverse socioeconomic profiles, thereby facilitating a comprehensive examination of vaccination outcomes. Furthermore, we propose the integration of socioeconomic status explicitly into our model via a welfare equation. As the COVID-19 pandemic evolves, the continual release of new data holds promise for refining the accuracy of our parameter estimates and simulations. Notably, the influence of COVID-19 variants remains unaddressed in our current model, a facet deserving of future investigation given its potential ramifications on virus transmission dynamics and disease severity.

Acknowledgements

We acknowledge the excellent comments of the anonymous reviewers, which have greatly improved the quality of the paper. We would like to thank the Intercollegiate Bio-mathematics Alliance's CURE (Cross-Institutional Undergraduate Research Experience) program for providing a platform that helped initiate this research project.

[Received: February 2023 — Accepted: May 2024]

References

Andreadakis, Z., Kumar, A., Román, R. G., Tollefsen, S., Saville, M. & Mayhew, S. (2020), 'The COVID-19 vaccine development landscape', *Nature Reviews. Drug Discovery* **19**(5), 305–306.

BBC News (2020), 'China's Covid vaccines: Who and how many people have been vaccinated?', `https://www.bbc.com/news/world-asia-china-55212787`. Accessed: 2021-07-12.

Brauer, F., Castillo-Chavez, C. & Castillo-Chavez, C. (2012), *Mathematical models in population biology and epidemiology*, Vol. 2, Springer.

Calafiore, G. C., Novara, C. & Possieri, C. (2020), 'A time-varying SIRD model for the COVID-19 contagion in Italy', *Annual Reviews in Control* **50**, 361–372.

Calleri, F., Nastasi, G. & Romano, V. (2021), 'Continuous-time stochastic processes for the spread of covid-19 disease simulated via a monte carlo approach and comparison with deterministic models', *Journal of Mathematical Biology* **83**(4), 34.

Carrillo-Larco, R. M. (2020), 'Covid-19 data sources in latin america and the caribbean', *Travel Medicine and Infectious Disease* **38**, 101750.

Castillo-Chavez, C. (2013), *Mathematical and statistical approaches to AIDS epidemiology*, Vol. 83, Springer Science & Business Media.

CDC (2020), 'COVID-19 pandemic planning scenarios'. https://www.cdc.gov/coronavirus/2019-ncov/hcp/planning-scenarios.html.

Centers for Disease Control and Prevention (2021*a*), 'New York: CDC - NCHS Pressroom', https://www.cdc.gov/nchs/pressroom/states/newyork/ny.htm. Accessed: 2021-3-17.

Centers for Disease Control and Prevention (2021*b*), 'What You Should Know About the Possibility of COVID-19 Illness After Vaccination', https://archive.cdc.gov/. Accessed: 2021-08-09.

Central Intelligence Agency (2021), 'The World Factbook: Colombia - People and Society', https://www.cia.gov/the-world-factbook/countries/colombia/#people-and-society. Accessed: 2021-10-19.

Choi, Y., Kim, J. S., Kim, J. E., Choi, H. & Lee, C. H. (2021), 'Vaccination prioritization strategies for covid-19 in korea: a mathematical modeling approach', *International Journal of Environmental Research and Public Health* **18**(8), 4240.

Chowell, G., Diaz-Duenas, P., Miller, J., Alcazar-Velazco, A., Hyman, J., Fenimore, P. & Castillo-Chavez, C. (2007), 'Estimation of the reproduction number of dengue fever from spatial epidemic data', *Mathematical Biosciences* **208**(2), 571–589.

Cintrón-Arias, A., Castillo-Chávez, C., Betencourt, L., Lloyd, A. L. & Banks, H. T. (2008), The estimation of the effective reproductive number from disease outbreak data, Technical report, North Carolina State University. Center for Research in Scientific Computation.

CoronaTracker (2021), 'Colombia COVID-19 Statistics', https://www.worldometers.info/coronavirus/country/colombia/. Accessed: 2021-10-24.

COVID19 Vaccine Tracker (2021), 'Colombia: The Latest on COVID-19 Vaccine Development and Distribution', https://covid19.trackvaccines.org/country/colombia/. Accessed: 2021-10-24.

DePietro, A. (2021), 'U.s. poverty rate by state in 2021', https://www.forbes.com/sites/andrewdepietro/2021/11/04/us-poverty-rate-by-state-in-2021/?sh=205544c21b38. Accessed: 2022-1-30.

Google News (2021), 'COVID-19 Map', https://news.google.com/covid19/map?hl=en-US&mid=%2Fm%2F02_286&gl=US&ceid=US%3Aen. Accessed: 2021-11-7.

Jentsch, P. C., Anand, M. & Bauch, C. T. (2021), 'Prioritising covid-19 vaccination in changing social and epidemiological landscapes: a mathematical modelling study', *The Lancet Infectious Diseases* **21**(8), 1097–1106.

Katella, K. (2021), 'Comparing the covid-19 vaccines: How are they different?'. https://www.yalemedicine.org/news/covid-19-vaccine-comparison

Keno, T. D. & Etana, H. T. (2023), 'Optimal control strategies of covid-19 dynamics model', *Journal of Mathematics* **2023**, 1–20.

Kerekes, S., Ji, M., Shih, S.-F., Chang, H.-Y., Harapan, H., Rajamoorthy, Y., Singh, A., Kanwar, S. & Wagner, A. L. (2021), 'Differential effect of vaccine effectiveness and safety on covid-19 vaccine acceptance across socioeconomic groups in an international sample', *Vaccines* **9**(9), 1010.

Kermack, W. O. & McKendrick, A. G. (1927), 'A contribution to the mathematical theory of epidemics', *Proceedings of the Royal Society of London. Series A, Containing papers of a mathematical and physical character* **115**(772), 700–721.

Khan, A. A., Ullah, S. & Amin, R. (2022), 'Optimal control analysis of covid-19 vaccine epidemic model: a case study', *The European Physical Journal Plus* **137**(1), 1–25.

Khan, A., Hassan, M. & Imran, M. (2014), 'Estimating the basic reproduction number for single-strain dengue fever epidemics', *Infectious Diseases of Poverty* **3**, 1–17.

Le, T. T., Cramer, J. P., Chen, R. & Mayhew, S. (2020), 'Evolution of the COVID-19 vaccine development landscape', *Nature Reviews Drug Discovery* **19**(10), 667–668.

Macrotrends (2019), 'Colombia Poverty Rate 2008-2024', `https://www.macrotrends.net/countries/COL/colombia/poverty-rate#:~:text=Colombia%20poverty%20rate%20for%202019,a%200.1%25%20increase%20from%202017`. Accessed: 2022-1-30.

Martcheva, M. (2015), *An introduction to mathematical epidemiology*, Vol. 61, Springer.

Ministerio de Salud y Protección Social (2020), 'Colombia confirma su primer caso de covid-19'.

National Institute of Health (2021), 'COVID-19 in Colombia', `https://www.ins.gov.co/Noticias/Paginas/Coronavirus.aspx`.

Ndwandwe, D. & Wiysonge, C. S. (2021), 'COVID-19 vaccines', *Current Opinion in Immunology* **71**, 111–116.

Niño-Torres, D., Ríos-Gutiérrez, A., Arunachalam, V., Ohajunwa, C. & Seshaiyer, P. (2021), 'Stochastic modeling, analysis, and simulation of the COVID-19 pandemic with explicit behavioral changes in Bogotá: A case study', *Infectious Disease Modelling* .

Niño-Torres, D., Ríos-Gutiérrez, A., Arunachalam, V., Ohajunwa, C. & Seshaiyer, P. (2022), 'Stochastic modeling, analysis, and simulation of the covid-19 pandemic with explicit behavioral changes in bogotá: A case study', *Infectious Disease Modelling* **7**(1), 199–211.

NYC Department of City Planning (2022), 'NYC Population Facts', `https://www.nyc.gov/site/planning/planning-level/nyc-population/nyc-population.page`. Accessed: 2022-1-31.

NYC Department of Health (2021), 'COVID-19: Latest Data', https://www1.nyc.gov/site/doh/covid/covid-19-data.page. Accessed: 2022-1-26.

NYC Department of Health (2022*a*), 'COVID-19: Data on Vaccines', https://www1.nyc.gov/site/doh/covid/covid-19-data-vaccines.page. Accessed: 2022-1-26.

NYC Department of Health (2022*b*), 'COVID-19: Data Trends and Totals', https://www1.nyc.gov/site/doh/covid/covid-19-data-totals.page. Accessed: 2022-1-26.

Ogueda-Oliva, A. G., Martínez-Salinas, E. J., Arunachalam, V. & Seshaiyer, P. (2023), 'Machine learning for predicting the dynamics of infectious diseases during travel through physics informed neural networks', *Journal of Machine Learning for Modeling and Computing* **4**(3).

Our World in Data (2021), 'United States: COVID-19 Testing', https://ourworldindata.org/coronavirus/country/united-states#how-many-tests-are-performed-each-day. Accessed: 2021-11-7.

Our World in Data Colombia (2021), 'Coronavirus (COVID-19) Vaccinations', https://ourworldindata.org/covid-vaccinations?country=COL. Accessed: 2022-2-9.

Our World in Data USA (2021), 'Coronavirus (COVID-19) Vaccinations', https://ourworldindata.org/covid-vaccinations?country=USA. Accessed: 2022-2-9.

Padmanabhan, P., Seshaiyer, P. & Castillo-Chavez, C. (2017), 'Mathematical modeling, analysis and simulation of the spread of Zika with influence of sexual transmission and preventive measures', *Letters in Biomathematics* **4**(1), 148–166.

Reuters (2021*a*), 'Colombia: The latest coronavirus counts, charts and maps', https://graphics.reuters.com/world-coronavirus-tracker-and-maps/countries-and-territories/colombia/. Accessed: 2021-10-24.

Reuters (2021*b*), 'Guest view: Colombia's struggle against poverty', https://www.reuters.com/breakingviews/guest-view-colombias-struggle-against-poverty-2021-05-11/. Accessed: 2022-1-30.

Rosenberg, E. S., Dorabawila, V., Easton, D., Bauer, U. E., Kumar, J., Hoen, R., Hoefer, D., Wu, M., Lutterloh, E., Conroy, M. B. et al. (2022), 'Covid-19 vaccine effectiveness in new york state', *New England Journal of Medicine* **386**(2), 116–127.

Sadri, K., Aminikhah, H. & Aminikhah, M. (2023), 'A mathematical system of COVID-19 disease model: Existence, uniqueness, numerical and sensitivity analysis', *MethodsX* **10**, 102045.

Salgado, M. R. M., Salgado, R. & Anand, R. (2022), *South Asia's path to resilient growth*, International Monetary Fund.

Silver, C. (2021), 'The new york city recovery index', https://www.investopedia.com/new-york-city-nyc-economic-recovery-index-5072042. Accessed: 2021-10-11.

Statista (2021), 'COVID-19 Transmission Rate in the U.S. by State', https://www.statista.com/statistics/1119412/covid-19-transmission-rate-us-by-state/. Accessed: 2021-1-31.

Tchoumi, S. Y., Schwartz, E. J. & Tchuenche, J. M. (2024), 'A deterministic model of COVID-19 with differential infectivity and vaccination booster', *Decision Analytics Journal* **10**, 100374.

Unidad de salud (2021), 'Gobierno definió fecha de inicio de vacunación y compra de más dosis', https://www.eltiempo.com/salud/vacunacion-en-colombia-inicia-el-20-de-febrero-asi-lo-aseguro-el-presidente-ivan-duque-563557. Accessed: 2022-1-30.

Van Rossum, G. & Drake, F. L. (2009), *Python 3 Reference Manual*, CreateSpace, Scotts Valley, CA.

Virtanen, P., Gommers, R., Oliphant, T. E., Haberland, M., Reddy, T., Cournapeau, D., Burovski, E., Peterson, P., Weckesser, W., Bright, J., van der Walt, S. J., Brett, M., Wilson, J., Millman, K. J., Mayorov, N., Nelson, A. R. J., Jones, E., Kern, R., Larson, E., Carey, C. J., Polat, İ., Feng, Y., Moore, E. W., VanderPlas, J., Laxalde, D., Perktold, J., Cimrman, R., Henriksen, I., Quintero, E. A., Harris, C. R., Archibald, A. M., Ribeiro, A. H., Pedregosa, F., van Mulbregt, P. & SciPy 1.0 Contributors (2020), 'SciPy 1.0: Fundamental Algorithms for Scientific Computing in Python', *Nature Methods* **17**, 261–272.

Wang, Y., Lu, G. & Du, J. (2022), 'Calibration and prediction for the inexact sir model', *Mathematical Biosciences and Engineering* **19**(3), 2800–2818.

Watson, O. J., Barnsley, G., Toor, J., Hogan, A. B., Winskill, P. & Ghani, A. C. (2022), 'Global impact of the first year of COVID-19 vaccination: a mathematical modelling study', *The Lancet Infectious Diseases* **22**(9), 1293–1302.

World Health Organization (2021), 'WHO Coronavirus (COVID-19) Dashboard: Colombia', https://covid19.who.int/region/amro/country/co. Accessed: 2021-10-24.

World's Capital Cities (2022), 'Capital Facts for Bogota, Colombia', https://colombia.travel/en/bogota. Accessed: 2022-1-31.

Yaladanda, N., Mopuri, R., Vavilala, H. P. & Mutheneni, S. R. (2022), 'Modelling the impact of perfect and imperfect vaccination strategy against SARS CoV-2 by assuming varied vaccine efficacy over india', *Clinical Epidemiology and Global Health* **15**, 101052.

Yang, B., Yu, Z. & Cai, Y. (2022), 'The impact of vaccination on the spread of covid-19: Studying by a mathematical model', *Physica A: Statistical Mechanics and its Applications* **590**, 126717.

Yoshida, N. (2023), 'Existence of exact solution of the susceptible-exposed-infectious-recovered (SEIR) epidemic model', *Journal of Differential Equations* **355**, 103–143.

Zhang, S., Ponce, J., Zhang, Z., Lin, G. & Karniadakis, G. (2021), 'An integrated framework for building trustworthy data-driven epidemiological models: Application to the COVID-19 outbreak in New York City', *PLoS Computational Biology* **17**(9), e1009334.